Broadband tunable single-frequency Nd:YVO_4/LBO green laser with high output power

Wenzhe Wang, Huadong Lu,* Jing Su, and Kunchi Peng

State Key Laboratory of Quantum Optics and Quantum Optics Devices, Institute of Opto-Electronics, Shanxi University, Taiyuan 030006, China

*Corresponding author: luhuadong@sxu.edu.cn

Received 18 September 2012; revised 25 November 2012; accepted 19 December 2012; posted 5 March 2013 (Doc. ID 176459); published 4 April 2013

We present a diode-pumped broadband tunable single-frequency and frequency-doubling Nd:YVO_4/LBO laser with high output power of 10.5 W in all tuning ranges around 532 nm. An etalon placed inside the resonator and the laser gain medium in a wedge shape are used for the coarse- and fine-tuning elements, respectively. By independently scanning the temperatures of the two tuning elements, broadband tunable ranges of 12 and 24 GHz have been achieved, respectively, for the fundamental and the second-harmonic waves. © 2013 Optical Society of America

OCIS codes: 140.3600, 140.3515, 140.3560, 140.3570.

1. Introduction

Diode-pumped and intracavity-doubled single-frequency green lasers have good beam quality and coherence, and have been extensively applied in scientific and technical fields, such as optical frequency standards, high-resolution laser spectroscopy, and so on [1,2]. Compared with fiber-based green lasers, diode-pumped tunable solid-state green lasers have lower intensity noise, which is preferred by most users [3]. High-power solid single-frequency green lasers are also used as the pump sources for Ti:sapphire lasers [4] and optical parameter oscillators [5]. In many applications, single-frequency green lasers with both broad tunable range and high output power are desired. For example, for spectroscopy applications of molecular iodine with the transition of 532.245 nm and I_2-stabilized laser systems, single-frequency green radiation around 532 nm with high output power above several watts and a significant tuning range over 10 GHz are required. High-power single-frequency green lasers using the ring cavity geometry were reported by several groups [6–8]. Broadband rapid tuning of diode-pumped neodymium (Nd) lasers was achieved by controlling the laser cavity length using piezo-electric [9], electro-optic [10], and audio-optic effects [11], respectively. Using the above techniques, the laser frequency can be scanned over a single-longitudinal mode (SLM), and in order to obtain frequency scan ranges of 1 GHz, a miniature resonator has to be selected. However, the strong mode hopping and mode competition in the miniature cavity possibly result in the multimode oscillation of high-power lasers and thus the single-frequency operation can be realized only at low-power levels. Taira *et al.* [12] investigated a tunable Nd microchip laser tuned over a wide frequency range of 107 GHz by shifting the gain crystal temperature. In this microchip design, the resonator was short enough, so its free spectrum range (FSR) was close to the gain bandwidth of the laser medium and only one cavity mode oscillated. But the short cavity length limited the output power of the laser at the 103 mW level. A broadband tuning laser of 50 GHz with output power of about 600 mW was achieved by rotating the incidence angle of the intracavity etalon mounted on a galvanometer [13]. The diode-pumped tunable single-frequency Nd:YVO_4 laser with output power of 480 mW and tuning range of 17.2 GHz was

1559-128X/13/112279-07$15.00/0

demonstrated, in which two lithium niobate ($LiNbO_3$) crystals were utilized as the etalon and the fine-tuning element, respectively [14]. Murdoch *et al.* described a continuous-wave (CW) mode-hop-free tunable SLM Nd:YVO_4 laser with 25 W output power at 1064 nm [15], which was based on proven 532 nm laser technology [16]. In [15], the mode hopping of the fundamental wave in the resonator was suppressed and the SLM output at the fundamental frequency was achieved by inserting an intracavity second-harmonic-generation (SHG) crystal that converted a fraction of the intracavity power to the second-harmonic frequency intentionally. It has been proven in [15,16] that the lasing mode only experienced half of the nonlinear losses of the nonlasing modes and the loss difference between the lasing and the nonlasing modes was proportional to the intensity of the lasing mode. Therefore, the nonlinear crystal for SHG in a laser resonator can also serve as a mode-selection element, especially for a high-power laser. In the laser of [15], the tuning of the fundamental frequency was demonstrated by driving a tall piezoelectric transducer (PZT) stack and the tuning range of 3.2 GHz was achieved due to the limitation of the voltage applied to the PZT stack. Based on the scheme, a series of single-frequency tunable lasers with high output powers have been developed by Coherent Company. Output powers of 10, 12, and 18 W with a tunable range of 6.4 GHz for the green lasers at 532 nm are realized in Verdi 10, Verdi 12, and Verdi 18, respectively [16]. Friel *et al.* [17] achieved a single-frequency output of 250 mW with a tuning range of 17 GHz for a second-harmonic wave of 532 nm in an intracavity-doubled CW laser. The frequency-doubled Nd:YAG (Yb:YAG) laser using the KTP ($KTiOPO_4$, potassium titanyl phosphate) crystal as the temperature tuning element was completed by Okhapkin *et al.* [18,19], in which broad tunable ranges of 400 GHz (300 GHz) were obtained under output power of 250 mW at 532 nm (40 mW at 515.5 nm). In the above-mentioned solid lasers, the low damage thresholds of the $LiNbO_3$ and KTP crystals limited the output powers. To the best of our knowledge, the high-power broadband tunable diode-pumped green laser with both output power over 1 W and tunable range over 10 GHz has not be reported, thus far.

In this paper, we present a broadband tunable intracavity-doubled single-frequency solid green laser with high output powers over 10 W and 24 GHz tuning range, in which fused quartz with a high damage threshold serves as the etalon for coarse tuning in a large range, and the laser gain medium in a wedge shape is simultaneously used for the fine-tuning element. The paper is organized as follows: in Sections 2 and 3, the design and the frequency-tuning principles of the CW SLM laser are briefly analyzed, respectively. Then, the experimental setup is introduced in Section 4 and the experimental results are presented in Section 5. Finally, a conclusion is given in Section 6.

2. Design Characteristics of the CW SLM Green Laser

A ring resonator involving an optical diode is generally used in the design of solid-state SLM lasers, since in such traveling-wave resonators the harmful spatial hole-burning effect is eliminated and thus SLM operation can be possibly realized [20]. However, the stable SLM operation can be only achieved in low-power lasers if there is no other frequency selector to be inserted in the laser resonator due to the influence of mode competition [21]. For a high-power SLM laser, an etalon with FSR much larger than that of the resonator has to be utilized as a discriminator to narrow the effective gain bandwidth and increase the discrimination between the lasing mode and the nonlasing modes. In a ring laser cavity without the etalon, only a few longitudinal modes of the resonator close to the peak of the gain curve of the laser medium possibly oscillate prior to the other modes, which is the prominent advantage of the traveling-wave resonator over the standing-wave resonator [21]. For obtaining the real SLM operation, an etalon with large FSR is inserted into the ring cavity. The extra diffraction loss introduced by the etalon can suppress the oscillating of the nonlasing modes and thus the SLM laser can be obtained [7,21]. However, in this case, the laser can run at an SLM for only a short time (about few minutes), or else the stability of the SLM laser will be destroyed by the mode-hop phenomenon resulting from the slow drift of the length of the resonator [21]. To solve this problem, other technologies for the frequency stability have to be applied. In [15], a stable high-power SLM 1064 nm laser was achieved by inserting a nonlinear crystal into the resonator, which introduces different nonlinear losses between the lasing and the nonlasing modes. They proved that the lasing mode only experienced half of the nonlinear losses of the nonlasing modes; thus the lasing mode can be tuned in the frequencies away from the peak of the gain curve. In their laser, the frequency-tuning range of 3.2 GHz without mode hop was realized by driving a tall PZT adhering to a resonator mirror. Comprehensively applying the above technologies, our SLM green laser is designed as the configuration of a traveling-wave ring cavity including an optical diode and an etalon, in addition to a laser gain medium and a frequency-doubling crystal. Similar to [15], the nonlinear crystal placed in the resonator is also used for suppressing the nonlasing modes. However, in our laser, the inserted nonlinear crystal is not only utilized to stabilize the SLM operation of the laser, but also is applied as a frequency doubler. Compared with previous high-power SLM frequency-tunable lasers given in [15,16], the presented laser has the following characteristics:

1. An end face of the laser medium is cut in a wedge shape to suppress the oscillation of "O" polarized light. For a high-power intracavity SHG laser, the stability of the second-harmonic-wave output is possibly influenced by the high nonlinear conversion

efficiency, because the losses of the main polarization mode of the fundamental wave satisfying the phase-matching condition are much higher than those of other polarization modes. In this case, the depletion of the main mode during frequency upconversion will unavoidably increase the possibility of the oscillation of other unexpected polarization modes. For solving the problem, in our design an end face of the laser crystal (Nd:YVO_4) is cut in a wedge shape with a suitable angle (the angle depends on the pump power of the laser; see [8] for details) to serve as a polarizing beam splitter for suppressing the oscillation of unexpected polarization modes and enhancing the superiority of the main polarization mode in the mode competition. According to [8], for a pump power of 47 W used in our experiment, the calculated minimum wedge angle for suppressing completely the σ-polarization laser equals 1.2°, so we cut an end facet of the Nd:YVO_4 crystal in a wedge shape of $\alpha = 1.5°$ with respect to the c axis of the crystal and made its front facet parallel to the c axis, which is enough to suppress the oscillation of the unexpected σ-polarization mode and enhance the superiority of the π-polarization mode in the mode competition.

2. In this presented laser, a special astigmatism self-compensation scheme without an astigmatism compensator is utilized [22]; thus the stability and the output power of the laser are significantly improved. The thermal lens effect and the configuration of the ring resonator in solid-state lasers are two causes resulting in astigmatic distortions [22]. According to the astigmatism self-compensation scheme given in [22], the beam distortions introduced by the two types of the astigmatism can be mutually compensated by taking the c axis of the Nd:YVO_4 crystal in the tangential plane. We optimize the resonator parameters to make the thermal lens astigmatism and the ring cavity astigmatism mutually compensating (see [22] for details). The thermal focal lengths in the tangential and sagittal planes are 150 and 100 mm, respectively, under a pump power of 47 W, and they are measured using the method presented by Hardman *et al.* [23]. In this case, when the angle of incidence on the resonator mirrors is 10°, the astigmatism introduced by the thermal lens can be basically compensated by the ring cavity astigmatism. The self-compensation of astigmatisms not only increases the stability range of the laser, but also reduces the intracavity loss and the difference of the beam size in the tangential and sagittal planes, which results in a wide stable range of laser operation (see Fig. 3 in [22]). Therefore, the astigmatism self-compensation enhances the stability of the laser and further improves the profile of the fundamental mode laser, which is necessary for realizing highly efficient mode matching and frequency doubling.

3. Frequency-Tuning Principle

In order to achieve the frequency tuning of the green laser, a temperature-controlled etalon is inserted into the resonator, which implements the coarse frequency tuning via temperature scanning. The differentiation of the laser wavelength with respect to the temperature of the etalon is expressed as [12]

$$\frac{d\lambda}{dT} = \lambda\left(\frac{1}{n_0}\frac{\partial n_0}{\partial T} + \frac{1}{l_0}\frac{\partial l_0}{\partial T}\right) = \lambda\left(\frac{\gamma_0}{n_0} + \alpha_0\right), \quad (1)$$

where, n_0 and l_0 are the refractive index and the length of the etalon, respectively, $\gamma_0 = \partial n_0/\partial T$ is the temperature coefficient of the refractive index, $\alpha_0 = \partial l_0/(l_0 \times \partial T)$ is the coefficient of thermal expansion, λ is the average wavelength of the laser, and T is the temperature of the etalon. The laser wavelength changes linearly when the temperature of the etalon is scanned and the tuning range depends on the values of γ_0 and α_0.

On the other hand, in order to obtain the continuously and finely tunable laser spectrum, we precisely adjust the optical path of the laser inside the resonator by slowly scanning the temperature of the gain medium. The differentiation of the laser wavelength versus the temperature of the gain medium depends on the following formula [12]:

$$\frac{d\lambda}{dT} = \lambda\left(\frac{l_1}{L}\frac{\partial n_1}{\partial T} + \frac{n_1}{L}\frac{\partial l_1}{\partial T}\right) = \lambda\left(\gamma_1\frac{l_1}{L} + \alpha_1\frac{l_1 n_1}{L}\right), \quad (2)$$

where λ is the laser wavelength, L is the length of the resonant cavity, and n_1, l_1, and T are the refractive index, the length, and the temperature of the laser crystal, respectively.

By tuning the temperature of the etalon, we can coarsely select a longitudinal mode around the required wavelength from the many possible longitudinal-resonator modes included in a transmission cycle of the etalon. Then precise and continuous frequency tuning around the selected longitudinal mode can be realized by slowly tuning the temperature of the laser medium.

The etalon and the wedge-shaped laser crystal are two independent tuning elements, and their temperature can be independently scanned. The etalon is used for coarsely mode selecting, and the laser crystal is used for finely and continually frequency tuning. Once the required frequency region is selected by the etalon, the temperature of the etalon is kept unchanging, and then the laser frequency can be continually tuned by slowly changing the temperature of the laser crystal without mode hopping within an FSR of the laser. When both temperatures of the etalon and the laser medium are fixed, the laser can stably operate at a chosen frequency for a long time of more than 10 h.

4. Laser Configuration and Experimental Setups

The configuration of the presented all-solid-state tunable green laser is shown in Fig. 1. The pump source is a CW fiber-bundled laser diode (LD) with a maximum output power of 60 W (LIMO60-F400-DL, 808EX1126, LIMO Lissotschenko Mikrooptik

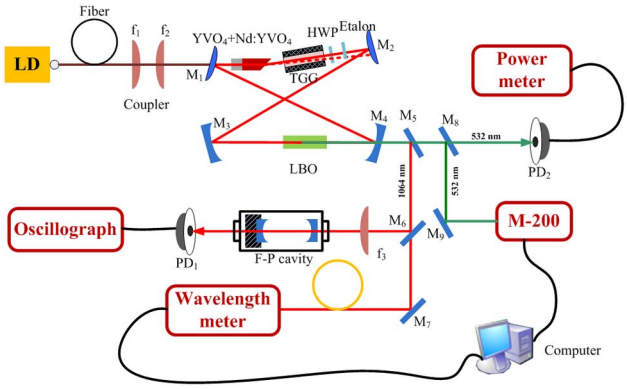

Fig. 1. (Color online) Experimental setup of the tunable single-frequency green laser.

GmbH). The diameter and the numerical aperture (NA) of the output coupling fiber are 400 μm and 0.22, respectively. The output beam of the LD is coupled into the laser resonator and is focused at the center of the gain medium. The optical coupler is a telescope system consisting of the lenses f_1 and f_2 with focal lengths of 30 and 80 mm, respectively. The waist diameters of the pump light and the produced fundamental mode laser are 1066 and 820 μm, respectively, which are in accordance with the requirement of the size ratio between the pump and the laser field [24]. A figure-eight-shaped ring resonator is constructed by four cavity mirrors (M_1–M_4). The input coupler M_1 is a convex mirror coated with high reflective (HR) films for 1064 nm and antireflective (AR) films for 808 nm, and the cavity mirror M_2 is also a convex mirror coated with HR films for 1064 nm. The curvature radii of M_1 and M_2 are both 1500 mm. The cavity mirror M_3 is a plano-concave mirror of 100 mm curvature radius coated with HR films for 1064 nm. The output coupler M_4 is also a plano-concave mirror of 100 mm radius coated with HR films for 1064 nm and AR films for 532 nm. The gain medium of the laser is a composite YVO_4/Nd:YVO_4 (yttrium vanadate/Nd^{3+}-doped yttrium vanadate) rod of 20 mm length (including and undoped end cap of 5 mm, and an Nd-doped part of 15 mm, where the Nd concentration of 0.2% with a wedge end facet of $\alpha = 1.5°$). The Nd:YVO_4 crystal is cut along the a axis, the front end face of which is coated with AR films for wavelengths of both 1064 and 808 nm, the second end face being coated with AR films only for 1064 nm. Based on the large birefringent property of the Nd:YVO_4 crystal, we are only able to align the main mode (solid line shown in Fig. 1) of the laser to resonate in the resonator by adjusting its incident direction on the wedge-shaped end facet of the laser crystal and to suppress those unexpected modes (dashed line shown in Fig. 1) [8]. At the same time, the wedge-shaped end facet is also used for eliminating the influence of the etalon effect resulting from the two plano–plano faces of crystal on the frequency-tuning characteristics of the laser [25]. The nonlinear crystal for the intracavity frequency doubling is an LBO crystal with dimensions of 3 mm × 3 mm × 18 mm cut for implementing type-I noncritical phase matching, and it is placed at the position of the beam waist of the oscillating laser between M_3 and M_4. To maintain the unidirectional operation of the laser, an optical diode consisting of an 8 mm long terbium gallium garnet (TGG) rod surrounded by a magnetic field and an AR-coated half-wave plate (HWP) at 1064 nm is applied. An uncoated temperature-controlled quartz etalon with a size of Φ10 × 0.5 mm inserted in the laser cavity is used for the mode selecting and frequency tuning. The effective finesse and the FSR of the uncoated etalon at 1064 nm are 0.6 and 207 GHz, respectively. The cavity length and the FSR of the laser resonator at 1064 nm are 486 mm, and 617 MHz, respectively.

The Nd:YVO_4 laser rod (the LBO crystal and the etalon) is placed in a closed copper block oven of 40 × 30 × 8 mm^3 (30 × 30 × 20 mm^3 and 15 × 15 × 4 mm^3) dimension with two small transparent glass windows at its two end faces for the laser going through. The temperature of the oven is controlled by a thermal electronic cooler (TEC, 9500/097/090B, Ferrotec Corporation) element attached on the oven, which is connected to a temperature controller. The temperature-controlling precision of the temperature controller (YG-DPSS FG-10 controller, Yuguang Co., Ltd.) based on the electronic proportional-integral-derivative (PID) technology is 0.03 K. By adjusting the electronic parameters of the PID, the temperature of the crystal in the oven can be controlled. For reducing the influence of the lasing thermal effect of the Nd:YVO_4 itself, the laser rod is tightly wrapped with indium foil, which contacts closely with the inside surface of the copper block oven for achieving good thermal conduction. There is the waterway, where the cooling water is circulated, on the copper block of the oven, which plays the role of the heat sink. A thermal probe (thermal sensitive resister) placed inside the oven and connected with the outside PID system is used for monitoring and measuring the temperature inside the oven. When thermal equilibrium is reached on a given power level, the measured temperature fluctuation is within 0.03 K. By adjusting the parameters of PID systems, the temperatures of the ovens of LBO crystal and the etalon are controlled at 421 K (the phase-matching temperature of LBO crystal) and 314 K, respectively. Although the thermal probe placed inside the oven does not directly touch on the crystal, but the oven is quite small, we may consider that the temperature inside the oven is homogeneous and the measured temperature can express the temperature of the crystal under thermal equilibrium.

To maintain the laser operating stably and to protect it from environmental noises, the laser resonator is built in a firm and thoroughly closed whole cavity with a thick hard metal wall. All elements of the resonator are fixed on the inside of the metal wall, and

the two small windows on the cavity for the pump laser going in and the produced laser going out, respectively, are also closed by the transparent glass plates. A big TEC connected to a temperature controller is attached on the outside wall of the whole cavity to keep its temperature around 303 K for reducing the influence of the environmental temperature fluctuation. The scheme of the whole cavity temperature controlling provides a good environment for stable operation of the laser. When the room temperature changes from 293 to 313 K, the stability of the laser is not influenced.

The output fundamental wave and the second-harmonic wave are separated by a dichroic mirror M_5 coated with HR films for 1064 nm and AR films for 532 nm. A small part of the reflected 1064 nm laser from M_5 is introduced into a confocal Fabry–Perot (F–P) cavity (F-P-200, Yuguang Co., Ltd.) with an FSR of 375 MHz and a passband of ~3.75 MHz, which is used for measuring and monitoring the longitudinal mode of the laser. Another small portion is injected into a wavelength meter (WS6/765, High Finesse Laser and Electronic Systems) for measurement of the laser wavelength. A little green light leaked from M_5 is used for analysis of the beam quality by means of a quality analyzer (M^2 – 200, Spiricon Inc.), and the retained part is detected by a power meter (LabMax-Top, Coherent Inc.).

5. Experimental Results and Analysis

The function curve of the output power for the single-frequency green laser versus the absorbed pump power is plotted in Fig. 2. Generally, the thermal effect in the laser medium and the nonlinear crystal limits further enhancement of the pump power of a laser and thus restricts the obtainable output power. In our design, by orienting the c axis of the Nd:YVO_4 crystal in the tangential plane (horizontal to optical table) of the ring cavity, the astigmatisms introduced by the thermal lens and the ring cavity can be mutually compensated [22]. Since the astigmatism compensator is not needed and thus the intracavity inserted losses are decreased, a higher optical conversion efficiency is achieved. The maximum output power of 10.7 W is measured under the pump power of 47 W, which is much larger than the threshold pump power of 27.5 W. (Note: for maintaining a longer lifetime of LD, higher pump powers have not been applied in the experiment.) The obtained optimal optical–optical conversion efficiency for the system is 22.8%. The long-term power stability of the laser recorded by a power meter is shown in Fig. 3. The power stability of the laser is better than $\pm 0.59\%$ for 10 h without mode hopping. The beam quality of the laser is measured by a M^2 meter, and the measured values of M_x^2 and M_y^2 are 1.10 and 1.18, respectively. The measurement result and the corresponding spatial beam profile are shown in Fig. 4 and its inset, respectively. The transmission curve of the fundamental wave through a scanned F–P cavity (Fig. 5) demonstrates that the laser operates in an SLM. The frequency bandwidth of the output single-frequency green laser is 2.5 MHz, which is measured by means of a heterodyne beat signal between the green laser and a reference laser at a wavelength of about 532 nm with a linewidth of 150 kHz from a low-power green laser.

The coarse tuning of the laser is implemented by scanning the temperature of the quartz etalon. Figure 6 shows the experimental results (blue squares) and the theoretical prediction (red solid line) for the dependence of the laser oscillation frequency on the temperature of the etalon. When the temperature of the etalon is tuned from 314 to 328 K, the wavelength of the fundamental wave around 1064 nm is upward tuned from 1064.4776 to 1064.5234 nm. The wavelength tuning range of 0.0458 nm (corresponding to 12 GHz) for the fundamental wave is achieved, and thus the tuning range of 24 GHz for the second-harmonic wave is demonstrated. Substituting the physical parameters of the fused quartz etalon ($n_0 = 1.449633@1064$ nm, $\gamma_0 = 3.0 \times 10^{-6}$ K^{-1}, and $\alpha_0 = 5.0 \times 10^{-7}$ K^{-1}) into

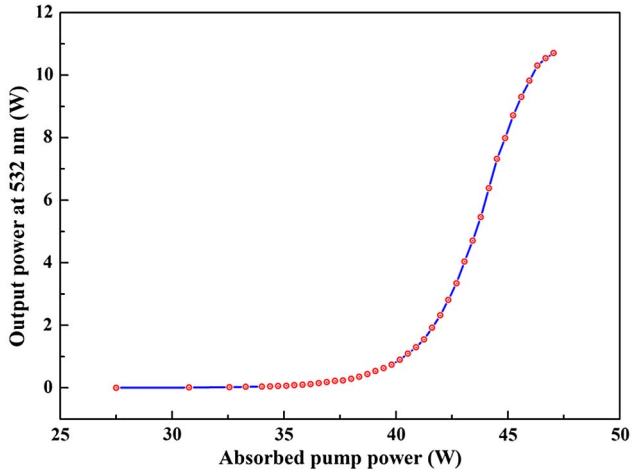

Fig. 2. (Color online) Output power of the single-frequency green laser versus pump power.

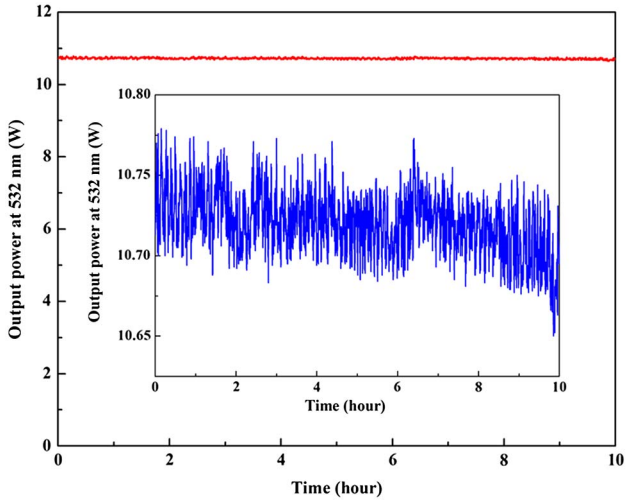

Fig. 3. (Color online) Power stability of the green laser in 10 h.

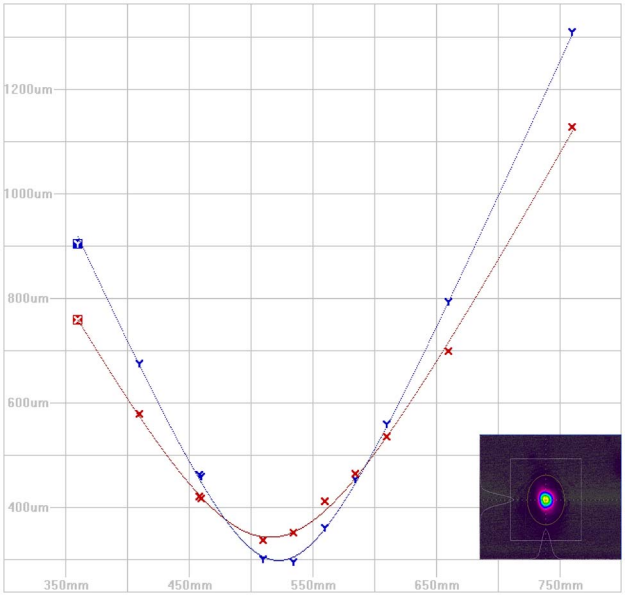

Fig. 4. (Color online) Measured M^2 values and the spatial beam profile for a 532 nm laser.

Eq. (1), the calculated tuning curve is shown in Fig. 6 (red solid line), which is in good agreement with the experimental measurements. Figure 7 shows the fluctuation of the output power within the tuning range of 24 GHz, which is quite small, and thus proves that the output powers over 10.5 W have been achieved totally within the tuning range.

In order to obtain the continuously and finely tunable laser spectrum, we precisely adjust the optical path of the laser inside the resonator by slowly scanning the temperature of the gain medium. Substituting the parameters of the Nd:YVO_4 crystal ($L = 486.5$ nm $n_1 = 2.1654@1064$ nm, $\gamma_1 = 1.04978 \times 10^{-5}$ K^{-1}, and $\alpha_1 = 11.37 \times 10^{-6}$ K^{-1}) into Eq. (2), we find that the continuously tunable range of the output green laser can reach an FSR of the laser resonator, i.e., 0.002235 nm (617 MHz), if the

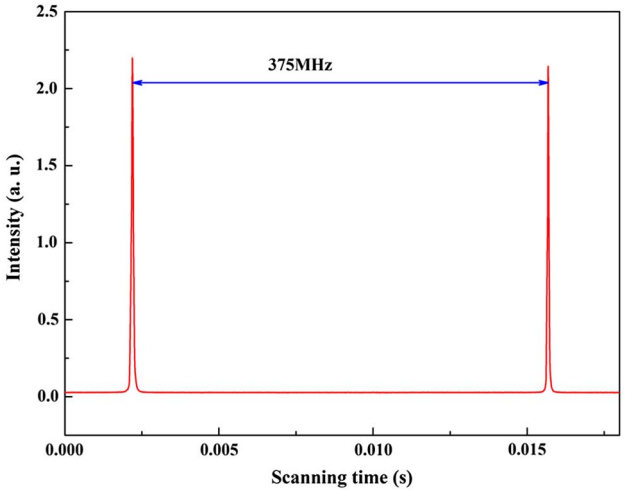

Fig. 5. (Color online) Laser transmission intensity obtained by scanning a confocal F–P cavity.

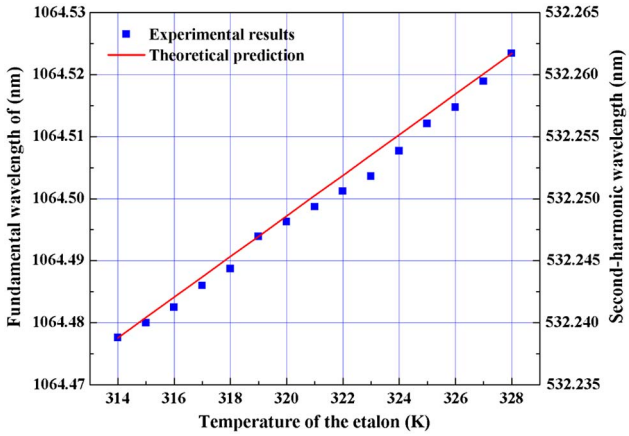

Fig. 6. (Color online) Wavelength of the fundamental wave dependent on the temperature of the quartz etalon.

temperature of the laser crystal is changed about 3 K. A typical tuning characteristic of the temperature-controlled gain medium is shown in Fig. 8. It shows that the tuning range of the Nd:YVO_4 is 0.0023 nm (609 MHz) in the temperature scanning of 3 K, which is consistent with the calculated result in Eq. (2).

In our system, the tuning element (laser medium and etalon) is placed in a small oven, the temperature of which is well controlled by a temperature controller with a precision of 0.03 K; thus the homogeneity and stability of the temperature distribution on the element can be proven basically. However, since the process of the thermal balance in the oven is quite slow, the speed of the temperature tuning is relatively low. In our experiment a tuning speed of 1 K/5 s is applied.

In fact, the tuning range of 24 GHz is only a fraction of the lasing spectrum range of the Nd:YVO_4 crystal; thus we can choose a different temperature range of the etalon to satisfy the different frequency requirement. In this experiment, we determine the

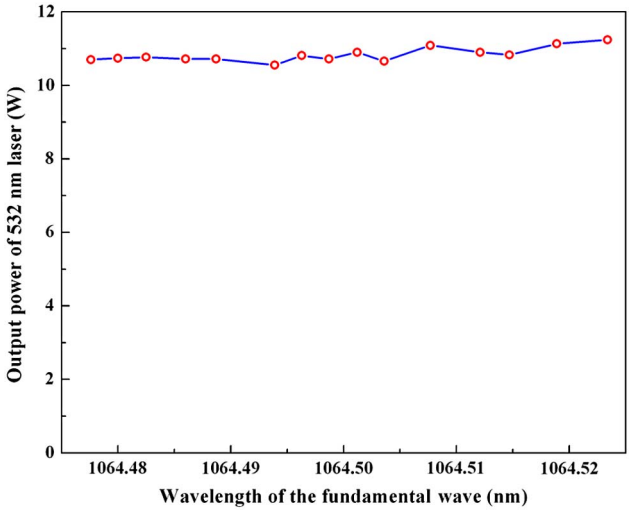

Fig. 7. (Color online) Laser output power versus fundamental wavelength during temperature scanning of etalon.

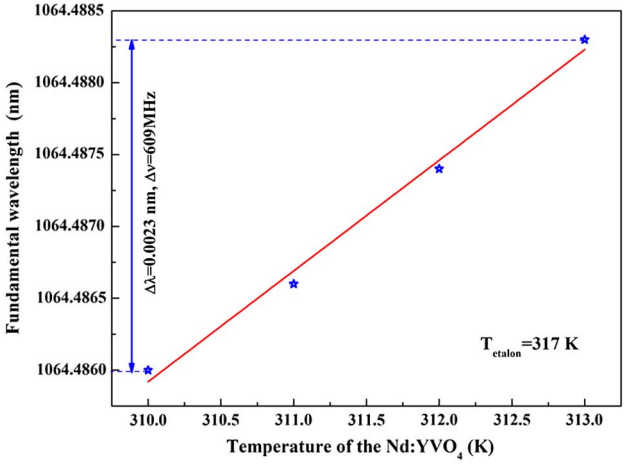

Fig. 8. (Color online) Fine tuning of the laser by changing the temperature of the laser medium for a given temperature of the etalon (317 K).

temperature of the etalon from 314 to 328 K, because the transition of the iodine molecule (532.245 nm) is in this range, which is required for our experiment.

6. Conclusions

In summary, a diode-pumped broadband tunable single-frequency green laser with high output power is demonstrated. In the presented laser, two tuning elements are applied. The intracavity quartz etalon is used for coarse tuning and selection of the frequency region, and the wedge-shaped gain medium is utilized to realize the fine and continual tuning. The tuning ranges for the fundamental and second-harmonic waves are 12 and 24 GHz, respectively. An output power of more than 10.5 W is achieved over the total frequency-tuning range. The tunable green laser in the wavelength range has some special applications; for instance, it can be used in the optical frequency standard based on the hyperfine peaks of molecular iodine, since its frequency-tuning range has covered several absorption lines of molecular iodine [1].

This research was supported by the National Basic Research Program of China (grant no. 2010CB923101), the NSFC Project for Excellent Research Team (grant no. 60821004), the National Major Scientific Equipment Developed Project of China (grant no. 2011YQ030127), and the National Natural Science Foundation of China (grant no. 61227015).

References

1. A. Arie and R. L. Byer, "Laser heterodyne spectroscopy of $^{127}I_2$ hyperfine structure near 532 nm," J. Opt. Soc. Am. B **10**, 1990–1997 (1993).
2. F. Hong, J. Ye, L. Ma, S. Picard, C. J. Borde, and J. L. Hall, "Rotation dependence of electric quadrupole hyperfine interaction in the ground state of molecular iodine by high-resolution laser spectroscopy," J. Opt. Soc. Am. B **18**, 379–387 (2001).
3. K. Liu, S. Cui, H. Zhang, J. Zhang, and J. Gao, "Noise suppression of single frequency fiber laser," Chin. Phys. Lett. **28**, 074211 (2011).
4. H. Lu, J. Su, C. Xie, and K. Peng, "Experimental investigation about influences of longitudinal-mode structure of pumping source on a Ti:sapphire laser," Opt. Express **19**, 1344–1353 (2011).
5. H. Vahlbruch, M. Mehmet, S. Chelkowski, B. Hage, A. Franzen, N. Lastzka, S. Gobler, K. Danzmann, and R. Schnabel, "Observation of squeezed light with 10 dB quantum-noise reduction," Phys. Rev. Lett. **100**, 033602 (2008).
6. K. I. Martin, W. A. Clarkson, and D. C. Hanna, "3 W of single-frequency output at 532 nm by intracavity frequency doubling of a diode-bar-pumped Nd:YAG ring laser," Opt. Lett. **21**, 875–877 (1996).
7. Y. Zheng, H. Lu, F. Li, K. Zhang, and K. Peng, "Four watt long-term stable intracavity frequency-doubling Nd:YVO_4 laser of single-frequency operation pumped by a fiber-coupled laser diode," Appl. Opt. **46**, 5336–5339 (2007).
8. Y. Zheng, F. Li, Y. Wang, K. Zhang, and K. Peng, "High-stability single-frequency green laser with a wedge Nd:YVO_4 as a polarizing beam splitter," Opt. Commun. **283**, 309–312 (2010).
9. A. Owyoung and P. Escherick, "Stress-induced tuning of a diode-laser-excited monolithic Nd:YAG laser," Opt. Lett. **12**, 999–1001 (1987).
10. P. A. Shultz and S. R. Henion, "Frequency-modulated Nd:YAG laser," Opt. Lett. **16**, 578–580 (1991).
11. D. C. Thompson, G. E. Busch, C. J. Hewitt, D. K. Remelius, T. Shimada, C. E. M. Strauss, C. W. Wilson, and T. J. Zaugg, "High-speed random access laser tuning," Appl. Opt. **38**, 2545–2553 (1999).
12. T. Taira, A. Mukai, Y. Nozawa, and T. Kobayashi, "Single-mode oscillation of laser-diode-pumped Nd:YVO_4 microchip lasers," Opt. Lett. **16**, 1955–1957 (1991).
13. J. Harrison, A. Finch, J. H. Flint, and P. F. Moulton, "Broadband rapid tuning of a single-frequency diode-pumped Neodymium laser," IEEE J. Quantum Electron. **28**, 1123–1130 (1992).
14. Y. Zheng, H. Lu, Y. Li, K. Zhang, and K. Peng, "Broadband and rapid tuning of an all-solid-state single-frequency Nd:YVO_4 laser," Appl. Phys. B **90**, 485–488 (2008).
15. K. M. Murdoch, D. A. Clubley, and M. J. Snadden, "A mode-hop-free tunable single-longitudinal-mode Nd:YVO_4 laser with 25 W of power at 1064 nm," Proc. SPIE **7193**, 71930 (2009).
16. Coherent Web site, http://www.coherent.com/Products/index.cfm?1852/Verdi-V-Series.
17. G. J. Friel, A. J. Kemp, T. K. Lake, and B. D. Sinclair, "Compact and efficient Nd:YVO_4 laser that generates a tunable single-frequency green output," Appl. Opt. **39**, 4333–4337 (2000).
18. M. V. Okhapkin, M. N. Skvortsov, A. M. Belkin, N. L. Kvashnin, and S. N. Bagayev, "Tunable single-frequency diode-pumped Nd:YAG ring laser at 1064/532 mm for optical frequency standard applications," Opt. Commun. **203**, 359–362 (2002).
19. M. V. Okhapkin, M. N. Skvortsov, N. L. Kvashnin, and S. N. Bagayev, "Single-frequency intracavity doubled Yb:YAG ring laser," Opt. Commun. **256**, 347–351 (2005).
20. K. C. Peng, L. A. Wu, and H. J. Kimble, "Frequency-stabilized Nd:YAG laser with high output power," Appl. Opt. **24**, 938–940 (1985).
21. F. A. Camargo, T. Z. Willette, T. Badr, N. U. Wetter, and J. J. Zondy, "Tunable single-frequency Nd:$YVO_4BiBI_3O_6$ ring laser at 671 nm," IEEE J. Quantum Electron. **46**, 804–809 (2010).
22. Y. J. Wang, Y. H. Zheng, Z. Shi, and K. C. Peng, "High-power single-frequency Nd:YVO_4 green laser by self-compensation of astigmatisms," Laser Phys. Lett. **9**, 506–510 (2012).
23. P. J. Hardman, W. A. Clarkson, G. J. Friel, M. Pollnau, and D. C. Hanna, "Energy-transfer upconversion and thermal lensing in high-power end-pumped Nd:YLF laser crystals," IEEE J. Quantum Electron. **35**, 647–655 (1999).
24. X. Peng, L. Xu, and A. Asundi, "Power scaling of diode-pumped Nd:YVO_4 lasers," IEEE J. Quantum Electron. **38**, 1291–1299 (2002).
25. J. Zhang, H. Ma, R. Wang, F. Li, C. Xie, and C. Peng, "All-solid-state single-frequency ring Nd:YVO_4 tunable lasers," Chin. J. Laser A **29**, 577–579 (2002).